SHOCK NANOSTRUCTURES IN LUNAR ZIRCON FROM APOLLO 15 AND 16: IMPLICATIONS FOR GEOCHRONOLOGY. Monika A. Kusiak[1] and Elizaveta Kovaleva[2], Dennis Vanderliek[3], Harry Becker[3], Franziska Wilke[2], Anja Schreiber[2] and Richard Wirth[2], [1]Institute of Geophysics Polish Academy of Sciences, Ksiecia Janusza 64, PL-01452 Warsaw, Poland, monika.kusiak@igf.edu.pl, [2]Helmholtz Centre Potsdam GFZ, 3.5 Interface Geochemistry, Telegrafenberg 1, 14473 Potsdam, Germany, [3]Institute for Geological Sciences, Freie Universität Berlin, Malteserstrasse 74-100, D-12249 Berlin, Germany

Introduction: Impact processes are ubiquitous in the Solar System, including the Moon. Zircon ($ZrSiO_4$), one of the most common accessory minerals, may show characteristic shock-related micro- and nano-structures, which can be indicative of the physicochemical conditions of impact processes [1,2,3,4]. However, many shock-related microstructures in lunar zircons and their mechanisms of formation are not well studied or understood [5,6].

Eight grains of zircon from lunar impact breccias 15455 (Apollo 15, dimict breccia), 67915 (Apollo 16, polymict impact breccia) and 67955 (brecciated cumulate crystallized from impact melt) earlier characterized petrographically and geochronologically [1,6,7] were selected for the study to recognize a range of shock-related nano-structures and to extend the limited database of lunar zircon textures.

Method: Focus Ion Beam (FIB) foils of 15-20 µm wide, 10-15 µm deep and 100 nm thick were prepared from zircon for transmission electron microscopy (TEM). Chemical composition of nanoparticles has been determined by Energy Dispersive X-ray Spectroscopy (EDS) analyses focusing an electron beam on the nanocrystal. Structural data (d_{hkl} spacing and the angles between adjacent lattice planes of mineral) were determined from electron diffraction patterns calculated by fast Fourier transform.

Results: A wide range of sometimes complex, shock-related features in zircon has been observed: (1) planar and non-planar fractures in anhedral grains, Fig. 1A; (2) 'columnar', porous zircon rims around baddeleyite cores, Fig. 1B; (3) granular textured zircon, usually containing various sub- µm-size inclusions of ZrO_2 (monoclinic baddeleyite and cubic zirconia), Fig. 1C; (4) inclusions of FeS and FeNi or Si-rich glass present at triple junctions of granular zircon and baddeleyite, Fig. 1D; (5) irregular patches of amorphous and nanocrystalline ('mosaic crystal') domains in zircon, Fig. 2; (6) locally-recrystallized (microcrystalline) domains of zircon, Fig. 2. Despite the presence of sub-micrometer-scale heterogeneities and a great variety of zircon microstructures, the studied grains from the three different breccias often show concordant U-Pb ages. Furthermore, they yield a relatively uniform $^{207}Pb/^{206}Pb$ age distribution ranging from 4210 to 4201 Ma (n=7), and only one granular zircon aggregate yields a resolvable younger $^{207}Pb/^{206}Pb$ age of 4168±18 Ma [4]. In contrast, all three samples display evidence for partial or complete resetting of their K-Ar and U-Pb phosphate systematics by the Imbrium impact (3.9 Ga) or younger impact events [8,9,10,11,12].

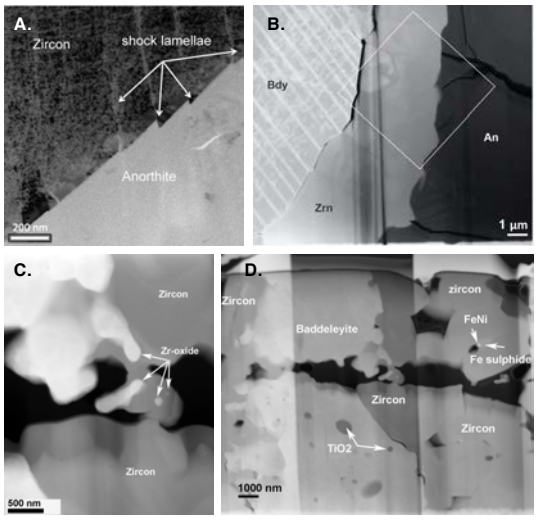

Figure 1. A. BF image of zircon interface with anothrite; B. HAADF Z-contrast image showing twin lamellae of baddeleyite (Bdy), columnar features of zircon and anorthite (An); C. HAADF TEM image with droplets of Zr-oxide; D. The overview HAADF TEM image showing the overview of zircon with monoclinic ZrO2 (baddeleyite) and inclusions of FeNi and Fe sulphide. Modified after Kusiak et al. (2022).

Discussion and Conclusions: Among the listed features, (1) and (6) can be attributed to the effect of shock wave propagation and shock deformation that led to partial amorphization of the zircon lattice, (2) and (3) are attributed to localized melting of silicates and reactions of SiO_2 rich melt (indicated by Si rich glass on triple junctions of zircon neoblasts) with relic baddeleyite triggered by shock heating, nanocrystalline (5) and recrystallized domains (6) reflect different states of post-shock annealing and recovery of the damaged lattices, metal alloy inclusions (4) may be inherited from the Mg suite parent melt the presence of traces of meteoritic material [1,6]. The ZrO_2 inclusions likely formed due to shock-induced decomposition and melting of preexisting zircon and subsequent

recrystallisation via the reaction between ZrO_2 and SiO_2. The visible ZrO_2 particles and SiO_2 glass at triple junctions are leftovers from that incomplete reaction.

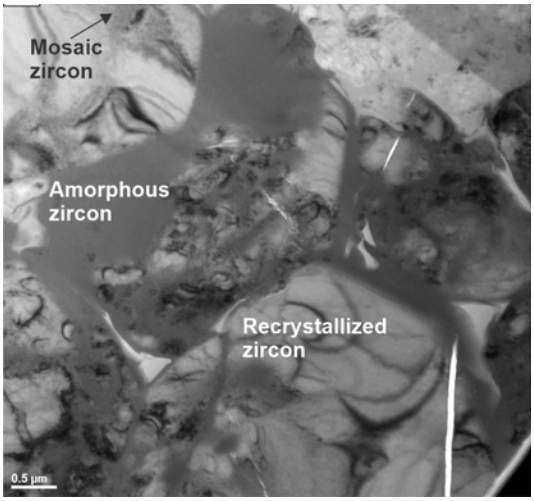

Figure 2. Various stages of zircon crystallinity; modified after Kusiak et al. 2022.

The different behavior of these chronometers relative to U-Pb zircon systematics in the same breccias indicate the robustness of zircons during impact processes [7]. What is surprising is that this conclusion is based on structurally very heterogeneous, partially amorphous zircon. The zircon structures and associated ancient ages either reflect a small time difference between solidification and recrystallization of different Zr phases, or the shock events were too brief to produce perceptible Pb loss during shock metamorphism.

References:

[1] Crow C.A., McKeegan K.D. and Moser D.E. (2017) *GCA, 202,* 264–284. [2] Grange M.L. et al. (2009) GCA, 73, 3093–3107. [3] Nemchin A.A. et al. (2009) Nat. Geosci, 2, 133–136. [4] Timms N.E. et al. (2012) MAPS 47, 120-141. [5] Kovaleva E. et al. (2021) *EPSL* 565, 116948. [6] Kusiak MA. et al. (2022) *CMP* 177, 112. [6] Norman M.D. and Nemchin A.A. (2014) EPSL 388, 387–398. [7] Vanderliek et al. (2021) *EPSL* 576, 11726. [8] Alexander Jr., E.C. and Kahl S. (1974) Lunar and Planetary Science Conference Proceedings, pp. 1353–1373. [9] Kirsten T., Horn P. and Kiko J. (1973) Lunar and Planetary Science Conference Proceedings, pp. 1757. [10] Marti K. et al. (1983) JGR, Solid Earth 88. [11] Vanderliek D.M. et al. (2021) Goldschmidt ttps://doi.org/10.7185/gold2021.6167. [12] Nemchin A.A. et al. (2021) Geochemistry 81, 125683.